# Plasma proteomic profiles of patients with HIV infection and coinfection with hepatitis B/C virus undergoing anti-retroviral therapy

CHEWAPORN TARNATHUMMANAN[1], THANAWAN SOIMANEE[2], JANYA KHATTIYA[2], WARISARA SRETAPUNYA[3], NARUMON PHAONAKROP[4], SITTIRUK ROYTRAKUL[4] and CHAREEPORN AKEKAWATCHAI[2,5]

[1]Graduate Program in Medical Technology, Faculty of Allied Health Sciences, Thammasat University, Pathumthani 12121, Thailand; [2]Thammasat University Research Unit in Diagnostic Molecular Biology of Chronic Diseases Related to Cancer, Pathumthani 12121, Thailand; [3]Department of Medical Technology and Pathology, Nakorn Nayok Hospital, Nakorn Nayok 26000, Thailand; [4]Functional Proteomics Technology Laboratory, National Center for Genetic Engineering and Biotechnology, National Science and Technology Development Agency, Pathumthani 12120, Thailand; [5]Department of Medical Technology, Faculty of Allied Health Sciences, Thammasat University, Klongluang, Pathumthani 12121, Thailand

Received March 2, 2024; Accepted July 26, 2024

DOI: 10.3892/br.2024.1843

**Abstract.** Chronic liver disease is becoming a leading cause of illness and mortality in patients living with human immunodeficiency virus (HIV; PLWH) undergoing suppressive anti-retroviral therapy. Its primary etiology is coinfection with hepatitis B and C virus (HBV and HCV, respectively). Chronic liver inflammation and fibrosis can potentially lead to the development of hepatocellular carcinoma (HCC). Therefore, monitoring of the disease progression in PLWH is required. The present study aimed to explore plasma protein profiles of PLWH and those coinfected with HBV and HCV using shotgun proteomics. HIV-monoinfected, HIV/HBV-coinfected, HIV/HCV-coinfected and uninfected control individuals were recruited. Patients in the three virus-infected groups had significantly higher levels of liver fibrosis indices (fibrosis-4 score and aspartate aminotransferase to platelet ratio index) compared with the control group. Liquid chromatography-tandem mass spectrometry analysis of plasma samples identified 1,074 proteins that were differentially expressed, where subsequent partial least squares-discriminant analysis model demonstrated clear clustering of proteomes from the four sample groups; 18 proteins that were significantly differentially expressed. Heatmap analysis identified two main groups of proteins, six proteins being upregulated only in the HIV/HBV-coinfection group and 10 proteins downregulated in all three virally infected groups. STITCH 5.0 analysis predicted an interaction network containing two identified proteins in the latter group, specifically ubiquitin interaction motif-containing 1 (UIMC1) and haptoglobin (HP), which are part of the profibrogenic TGF-1β/SMAD, inflammatory TNF and tumor suppressor BRCA1 pathways. Expression levels of UIMC1 and HP were significantly lower in HIV-infected groups compared with those in uninfected controls. Altogether, these proteomics data provide protein expression profiles potentially associated with HIV infection and coinfection with HBV/HCV, which may be applied to predict progression to advanced liver disease or HCC in PLWH.

*Correspondence to:* Dr Chareeporn Akekawatchai, Department of Medical Technology, Faculty of Allied Health Sciences, Thammasat University, 99 Moo 18, Klongluang, Pathumthani 12121, Thailand
E-mail: ejareepo@tu.ac.th

*Key words:* human immunodeficiency virus, hepatitis B, hepatitis C, shotgun proteomics

## Introduction

Human immunodeficiency virus (HIV) infection is a major health issue globally, with ~39.0 million patients living with HIV (PLWH) and ~29.8 million PLWH accessing anti-retroviral therapy (ART) in 2022 (1). Effective ART has notably reduced the rates of acquired immunodeficiency syndrome (AIDS)-associated morbidity and mortality. HIV infection is considered to be a chronic disease in countries where ART is available and PLWH have longer life expectancy (2,3). However, since the introduction of combination ART, chronic liver disease (CLD) has become a key concern in PLWH. The persistently low levels of viremia during ART can cause chronic hepatic injury and inflammation, potentially leading to hepatocellular carcinoma (HCC) development (3,4). To the best of our knowledge, there have only been three cohort studies that investigated HCC in PLWH populations (5-7). Clinical vigilance of CLD and HCC in PLWH is suggested (8).

Coinfection with hepatotropic hepatitis B and C virus (HBV and HCV, respectively) is a major cause of CLD in

PLWH receiving ART (9,10). HIV infection alone can cause liver steatosis and fibrosis (11-13), which aggravate the damage caused by HBV and HCV to promote liver fibrosis and cirrhosis in patients coinfected with HBV and HCV (5,14-16). Different mechanisms underlying acceleration of this form of disease progression have been proposed: Hepatotropic virus infection has been reported to induce persistent immune activation and inflammation, which participate in progressive liver disease in PLWH receiving ART (3,9). In patients coinfected with HIV/HCV, elevated levels of certain immune activation and inflammatory biomarkers such as soluble CD14 and CD163, IL-6 and -8 and IFN-γ-inducible protein 10, which are associated with hepatocellular injury and severity of liver fibrosis, have been previously found (14,17). Distinct apoptosis and inflammatory marker profiles have also been observed in patients with HBV and HIV/HBV, indicating different mechanisms of immune activation and disease progression between these patients (18). Previous studies have also suggested that HIV potentiates HCV-induced fibrogenesis by activating the profibrogenic TGF-β pathways in hepatocyte and hepatic stellate cells (HSCs), resulting in excessive production of extracellular matrix protein type I collagen by HSCs (19,20). To the best of our knowledge, there is no evidence of TGF-β activation following HIV/HBV coinfection; however, TGF-β serum levels are elevated in patients with chronic hepatitis B and hepatitis B with liver cirrhosis compared with those in normal control individuals, potentially linking chronic hepatitis B with the severity of liver cirrhosis (21). While mechanisms for hepatic inflammation and fibrosis caused by HIV infection and coinfection with HBV and HCV have been previously documented (4,9), the precise molecular pathways underlying progression to advanced liver disease and HCC require further clarification.

Previous studies have reported relatively high prevalence of HBV (11.4%) and HCV (7.6%) coinfection and liver fibrosis in PLWH populations receiving suppressive ART (22,23). This suggests that PLWH may progress to advanced chronic liver disease and HCC, warranting investigations into the molecular changes that occur in PLWH receiving long-term ART. The present study aimed to explore proteomic profiles associated with HIV infection and coinfection with HBV and HCV in PLWH using shotgun proteomics. Patients infected with HIV and uninfected control individuals were recruited and non-invasively assessed for the degree of liver fibrosis. Plasma samples were subjected to proteomics analysis. The plasma protein profiles may be used to predict disease progression and provide potential biomarkers for CLD caused by HIV and hepatotropic HBV and/or HCV.

## Materials and methods

*Study population, clinical data and laboratory investigation.* A total of 186 patients with HIV (age, 18-86 years; 61.8% male and 38.2% female) attending the Antiretroviral Therapy Clinic in Nakorn Nayok Hospital, Nakorn Nayok (Thailand) from April 2014 to October 2020 were recruited into the present study. The inclusion criteria were as follows: i) Patients aged >18 years with documented HIV infection; ii) receiving suppressive ART for >6 months and iii) available blood samples and clinical data. Patients who consumed alcohol, herbal medicine and steroidal drugs, in addition to patients with active opportunistic infections, were excluded. The patients were divided into 150 HIV-moninfected patients, aged 18-86 years, 58.7% male and 41.3% female, 19 HBV-coinfected HIV patients, 29-58 years, 73.7% male and 26.3% female, and 17 HCV-coinfected HIV patients, aged 20-62 years, 76.5% male and 23.5% female. In total, 50 uninfected controls, aged 20-60 years, 40% male and 60% female, were recruited from Police General Hospital, Bangkok (Thailand) in November 2022. Inclusion criteria for controls were individuals aged >18 years with available blood samples and clinical data who were seronegative for HIV, HBV and HCV infection. Individuals with notable liver fibrosis, determined by fibrosis-4 (FIB-4) score >1.45 or aspartate aminotransferase (AST)-to-platelet ratio index (APRI) >0.5, were excluded (24-26). The present study protocol was approved by the Human Ethics Committee No. 3, Thammasat University, Pathumthani (Thailand; approval no. 116/2565) and the Certificated Biological Safety Committee of Thammasat University, Pathumthani, (Thailand, approve no. 079/2565).

Clinical and laboratory data of the HIV group were obtained and characterized as described in previous studies (22,23). Briefly, the data collected from the medical records of the patients were age, sex, $CD4^+$ cell count, HBV/HCV coinfection, levels of AST and alanine aminotransferases (ALT), platelet count, HIV viral load and ART regimen and duration. Anti-HIV, HBV surface antigen and anti-HCV tests were performed to recruit seronegative HIV, HBV and HCV-uninfected controls. The extent of liver fibrosis in HIV-infected patients and uninfected controls was evaluated by measuring non-invasive markers FIB-4 and APRI, which are commonly used scoring systems recommended for assessing liver fibrosis in the presenceof chronic HCV by the World Health Organization (27). FIB-4 score >1.45 or APRI >0.5 was considered to be significant liver fibrosis (24-26). Additionally, levels of fibrotic markers, namely laminin (LN), procollagen type III N-terminal peptide (PIIINP), hyaluronic acid (HA) and type IV collagen (IVC), in addition to tumor marker α-fetoprotein (AFP), were measured using electrochemiluminescence immunoassay according to the maufacturer's instructions (Mindray CL-900i using LN, PIIINP, HA, IVC and AFP test kits (cat. nos. LV111, PIIINP111, HA111, C IV111 and AFP111, respectively; all Mindray Medical International Co., Ltd.).

EDTA-blood samples left over from routine examination were collected from the clinical laboratory of Nakorn Nayok Hospital. Plasma was separated within 8 h of collection by centrifuging at 2,000 x g for 10 min at room temperature and stored at -80˚C until further use. Plasma samples from 186 patients infected with HIV were classified into the following three groups: HIV-monoinfection (n=150), HIV/HBV coinfection (n=19) and HIV/HCV coinfection (n=17). Blood samples from seronegative HIV, HBV and HCV individuals (n=50) with FIB-4 score ≤1.45 and APRI ≤0.5 were designated as uninfected controls. All samples were then subjected to proteomic analysis (Fig. 1).

*Sample preparation and liquid chromatography-tandem mass spectrometry (LC-MS/MS).* Total protein concentration in plasma samples was measured using the Lowry method, with bovine serum albumin applied as the standard (28).

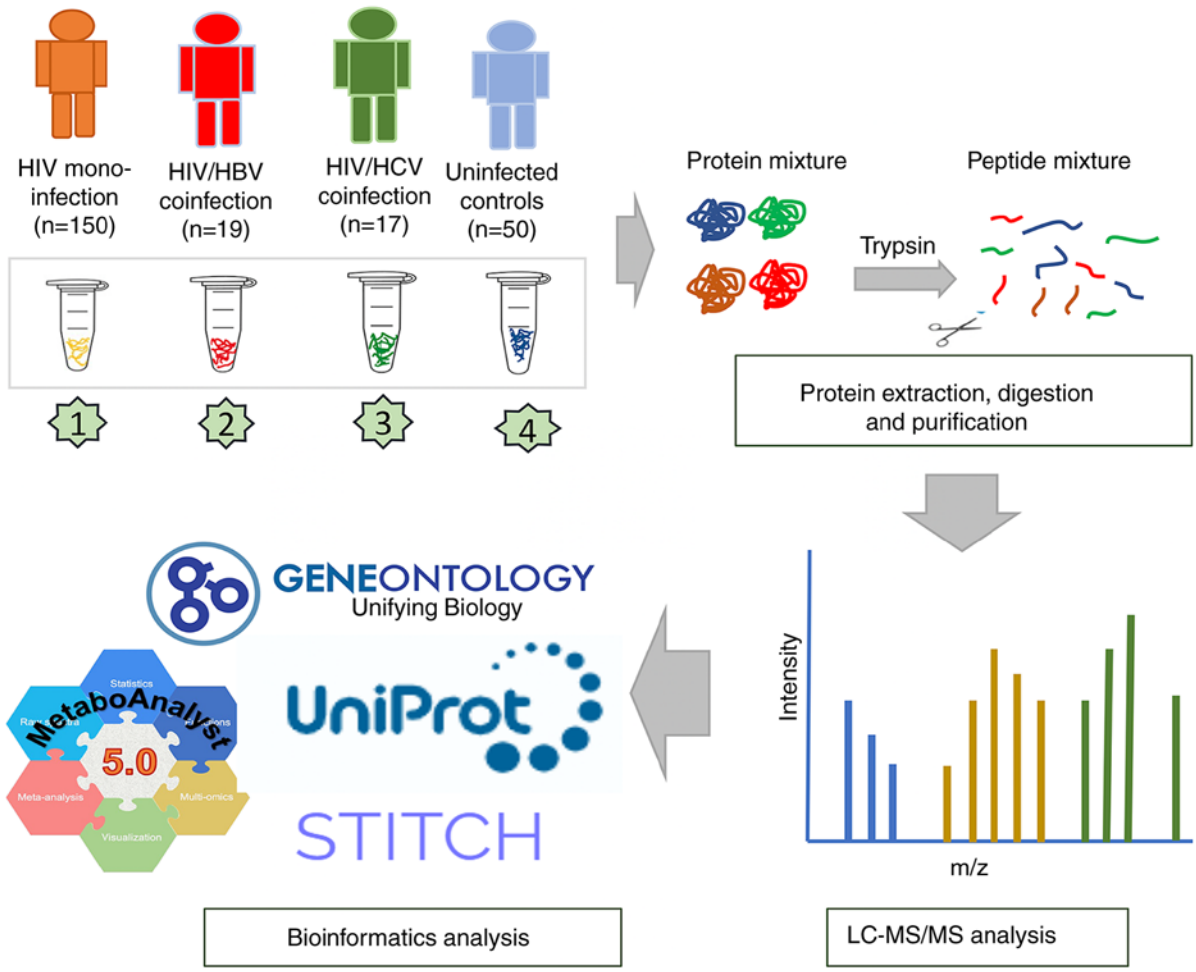


Figure 1. Experimental workflow in the present study. Serum samples from HIV-infected patients were subjected to protein extraion, digestion and purification before analyzed by LC-MS/MS. HIV, human immunodeficiency virus; HBV, hepatitis B virus; HCV, hepatitis C virus; LC-MS/MS, liquid chromatography-tandem mass spectrometry.

Protein samples were subjected to in-solution digestion. The samples, which were dissolved in 10 mM ammonium bicarbonate (AMBIC), underwent disulfide bond reduction using 5 mM dithiothreitol in 10 mM AMBIC at 60˚C for 1 h and alkylation of sulfhydryl groups using 15 mM iodoacetamide in 10 mM AMBIC at room temperature for 45 min in the dark, followed by digestion in porcine trypsin (Promega Corporation) in a 1:20 ratio at 37˚C overnight. Peptides were dried and resuspended with 0.1% formic acid prior to nano-LC-MS/MS analysis. The LC-MS/MS analysis was performed using an Ultimate 3000 Nano/Capillary LC System (Thermo Fisher Scientific, Inc.) coupled to a ZenoTOF 7600 mass spectrometer (SCIEX). Peptide separation was performed using a 75 $\mu$m x 15 cm column, packed with Acclaim PepMap RSLC C18 resin (2 $\mu$m, 100Å, nanoViper, Thermo Scientific, UK). The C18 column was maintained at 60˚C within a thermostatted column oven. Solvent A (0.1% formic acid in water) and solvent B (0.1% formic acid in 80% acetonitrile) were delivered to the analytical column. A gradient elution of 5-55% solvent B was employed to separate peptides at a constant flow rate of 0.30 $\mu$l/min over a 30-min period.

The electrospray ionization source was set in positive ion mode with an ion source temperature of 200˚C, spray voltage of 3300 V, curtain gas ($N_2$) of 35 psi, nebulizer gas of 50 psi, auxiliary heating gas of 55 psi, and declustering potential of 80 V. Top 50 most abundant precursor ions per survey MS1 for MS/MS with an intensity threshold exceeding 150 cps were selected. Precursor ions were dynamically excluded for 8 sec after two incidences of MS/MS sampling (with dynamic collision energy enabled). The MS2 spectra were collected in the range 350-1,800 m/z with a 250-ms accumulation time and Zeno trap enabled. The collision energy parameters included a declustering potential of 80 V, no DP spread, and a CE spread of 0 V. The time bins were summed (with all channels enabled) using a 150,000 cps Zeno trap threshold. The cycle time for the Top 50 DDA method was 3.0 sec. To minimize the effect of experimental variation, three independent LC-MS runs were performed for each sample.

*Protein identification and label-free quantification*. Proteins were quantified using MaxQuant 2.1.4.0 (Max-Planck Institute for Biochemistry) using the Andromeda search engine to match MS/MS spectra to the Uniprot *Homo sapiens* database (uniprot.org/) (29). Label-free quantification with MaxQuant's standard settings was performed as follows: i) Maximum of two missing cleavages; ii) mass tolerance of 0.6 Da for main search; iii) trypsin as a digesting enzyme; iv) carbamidomethylation

of cystein as fixed modification and v) oxidation of methionine and acetylation of the protein N-terminus as variable modifications. Peptides with ≥7 amino acids and ≥1 unique peptide were chosen for protein identification. Only proteins with ≥2 two peptides and ≥1 unique peptide were considered as being identified and subjected to further analysis. The false discovery rate (FDR) was set at 1% and estimated using the reversed search sequences. The maximal number of modifications/peptide was set to 5. The proteins present in the *H. sapiens* proteome were then downloaded from Uniprot as a search FASTA file. Potential contaminants in the contaminant FASTA files were added to the search space using the MaxQuant software.

*Data processing and bioinformatics analysis*. MaxQuant ProteinGroups.txt file was loaded into Perseus software version 1.6.6.0 (29) and potential contaminants that did not correspond to any Universal Proteomics Standard Set 1 (UPS1) protein were removed. Mass intensities were $\log_2$ transformed before pairwise comparisons using unpaired t tests. Missing values were imputed with a constant value (0) using the Perseus software. Intensity values of the MS/MS spectra were analyzed using partial least squares-discriminant analysis (PLS-DA) model, one-way ANOVA (P-value and FDR <0.05) and Kruskal-Wallis test using web-based tool MetaboAnalyst version 6.0 (metaboanalyst.ca/) (30,31). Heatmap analysis was performed by using the Morpheus online tool (software.broadinstitute.org/morpheus/) (32). Molecular function and subcellular localization of identified proteins were obtained from Gene Ontology (GO; geneontology.org/) and Uniprot databases (uniprot.org/). A protein-protein interaction network was constructed according to the STITCH 5.0 database (stitch.embl.de/).

*Statistical analysis*. Descriptive statistics were conducted to analyze characteristics of the study groups. Continuous variables are presented as median (range); categorical variables are reported as n (%). $\chi^2$ and Fisher's exact tests were used to determine the association between viral infection status and categorical variables, whereas the Kruskal-Wallis and Dunn's post hoc tests were performed to compare the median of continuous variables between study groups. P<0.05 was considered to indicate a statistically significant difference. SPSS for Windows version 18.0 (SPSS, Inc.) and GraphPad Prism 9.1.1 (Dotmatics) were used for the statistical analysis.

## Results

*Characteristics of the study population*. Table I demonstrates general and clinical characteristics of each group. All patients infected with HIV received suppressive ART for >6 months and had no detectable HIV viral load (data not shown), whereas no specific medications for HBV and HCV infection were used. All study groups had similar median ages, infected groups showed the higher male-to-female sex ratio than the uninfected control group. Although platelet counts of the three HIV-infected groups and uninfected group were not significantly different, medians of liver enzymes AST and ALT, in addition to the fibrosis markers FIB-4 and APRI, were significantly different. The additional analysis also indicated that the median values of AST, ALT, FIB-4 score and APRI in the three HIV-infected groups compared with the uninfected group differed significantly, excluding the FIB-4 score of HIV-mono-infection group. Differences in immune status and ART between the HIV-infected groups were also tested. Median levels of $CD4^+$ cell count and duration of ART in the HIV-monifected, HIV/HBV and HIV/HCV coinfected groups, were compared, yielding no statistical difference. ART drug regimens used in these three infected groups were not found to be significantly different (Table I).

There were higher FIB-4 scores and APRI in the three HIV-infected groups compared with the uninfected control group, except for the FIB-4 score in the HIV-monoinfected group (Fig. 2A and B). In addition, significantly higher FIB-4 score and APRI in the HIV/HCV group compared with the HIV-monoinfection group were observed. Key components of the extracellular matrix that typically accumulate during liver fibrosis, namely LN, IVC, PIIINP and HA, coupled with the tumor marker AFP (33), were examined in the plasma samples. HIV groups also had significantly higher levels of LN and IVC compared with the uninfected control group, except for LN levels in the HIV-monoinfection group (Fig. 2C and D). Consistent with FIB-4 score and APRI, LN and IVC levels were found to be significantly higher in the HIV/HCV group compared with HIV monoinfection. Notably, elevated plasma PIIINP, HA and AFP levels in the infected groups was not observed, whereas the HIV/HCV group had significantly higher levels of all of these markers compared with the HIV-monoinfection group (data not shown).

*Plasma proteomic profiles*. Shotgun proteomics was conducted to explore the plasma protein profiles. A total of 1,074 proteins were differentially expressed. PLS-DA model demonstrated clear separation of the proteome between sample groups, indicating significant differences in the plasma protein profiles (Fig. 3A). Of these, 18 were significantly differentially expressed (Fig. 3C; Table II). PLS-DA model of 18 selected proteins also indicated a clear clustering of proteins from the four sample groups (data not shown). Analysis for localization and function of the 18 proteins was conducted using GO and Uniprot databases (Fig. 3D and E). These proteins were primarily located in the nucleus (32.4%) and cytoplasm (29.4%) and in other intracellular and extracellular compartments (Fig. 3E). The cellular and molecular functions were enriched in molecular processes, including 'cell cycle, cell proliferation, cell differentiation and cell death' (15.4%), 'cell signaling' (11.5%), 'RNA processing and transport' (11.5%), 'binding protein' (11.5%), 'extracellular matrix protein and cytoskeleton' (11.5%), 'transcription' (7.7%), 'protein transport and degradation' (7.7%), 'cell adhesion and cell migration' (7.7%), 'inflammation, immune response and anti-viral activity' (7.7%) 'DNA replication and repair' (3.8%) and 'metabolic process' (3.8%; Fig. 3D).

Heatmap analysis demonstrated differential expression of the 18 selected proteins (Fig. 3B). A total of 10 proteins was downregulated in the HIV-monoinfected, HIV/HBV and HIV/HCV groups compared with those in the uninfected control group, included haptoglobin (HP), HBV X-transactivated gene 13 protein, forkhead-associated domain-containing protein 1, tenascin-X,

Table I. General and clinical characteristics of the patients infected with HIV and the uninfected control group recruited into the present study.

| Characteristic | Uninfected (n=50) | HIV (n=150) | P-value[c] | HIV/HBV (n=19) | P-value[c] | HIV/HCV (n=17) | P-value[c] | P-value[d] |
|---|---|---|---|---|---|---|---|---|
| Age (years)[a] | 44.5 (20.0-77.0) | 44.0 (18.0-86.0) | | 46.0 (29.0-58.0) | | 43.0 (20.0-62.0) | 0.965 | |
| Sex[b] | | | | | | | | 0.012 |
| Male | 20 (40) | 88 (58.7) | | 14 (73.7) | | 13 (76.5) | | |
| Female | 30 (60) | 62 (41.3) | | 5 (26.3) | | 4 (23.5) | | |
| Platelet count (x$10^3$ cells/$\mu$l)[a] | 274 (194-435) | 275.5 (34-922) | | 276 (110-387) | | 279 (133-447) | 0.816 | |
| Aspartate aminotransferase (U/l)[a] | 19 (6-52) | 26 (13-161) | <0.001 | 25 (17-168) | <0.001 | 37 (16-162) | <0.001 | |
| Alanine aminotransferase (U/l)[a] | 16 (4-167) | 24 (6-169) | 0.016 | 21 (9-111) | <0.001 | 32 (7-178) | <0.001 | |
| Fibrosis-4 score[a] | 0.74 (0.20-1.38) | 0.83 (0.23-9.57) | 0.057 | 0.99 (0.31-3.01) | 0.044 | 1.30 (0.28-3.94) | 0.001 | |
| Alanine aminotransferase to platelet ratio index[a] | 0.18 (0.06-0.38) | 0.23 (0.05-5.09) | <0.001 | 0.23 (0.13-1.77) | 0.004 | 0.53 (0.13-1.34) | <0.001 | |
| $CD4^+$ cell count (cells/$\mu$l)[a] | - | 550 (1-1,644) | | 365 (30-1,016) | | 421 (13-896) | 0.326 | |
| Duration of anti-retroviral therapy (months)[a] | - | 62.2 (6.0-169.0) | | 69.3 (6.1-308.4) | | 75.0 (6.7-156.5) | 0.351 | |
| Anti-retroviral drugs[b] | | | | | | | | 0.418 |
| Lamivudine/zidovudine/nevirapine | - | 34 (22.7) | | 2 (10.5) | | 1 (5.9) | | |
| Tenofovir-based | - | 86 (57.3) | | 13 (68.4) | | 12 (70.6) | | |
| Other regimens | - | 30 (20.00) | | 4 (21.1) | | 4 (23.5) | | |
| Nevirapine experience[b] | | | | | | | | 0.205 |
| Non-nevirapine-based regimen | - | 112 (75.6) | | 14 (73.7) | | 16 (94.1) | | |
| Nevirapine-based regimen | - | 33 (25.33) | | 5 (26.3) | | 1 (5.9) | | |

[a]Continuous data are shown as the median (range) and [c]P-values for median comparisons among the HIV-, HIV/HBV-, HIV/HCV-infected and uninfected control groups were calculated using the Kruskal-Wallis test and Dunn's post hoc test. [b]Categorical data are presented as number and percentage [n (%)] and [d]P-values for the comparisons of the three or four study groups were calculated using the $\chi^2$ and Fisher's exact tests. P<0.05 was considered to indicate a statistically significant difference. HIV, human immunodeficiency virus; HBV, hepatitis B virus; HCV, hepatitis C virus.

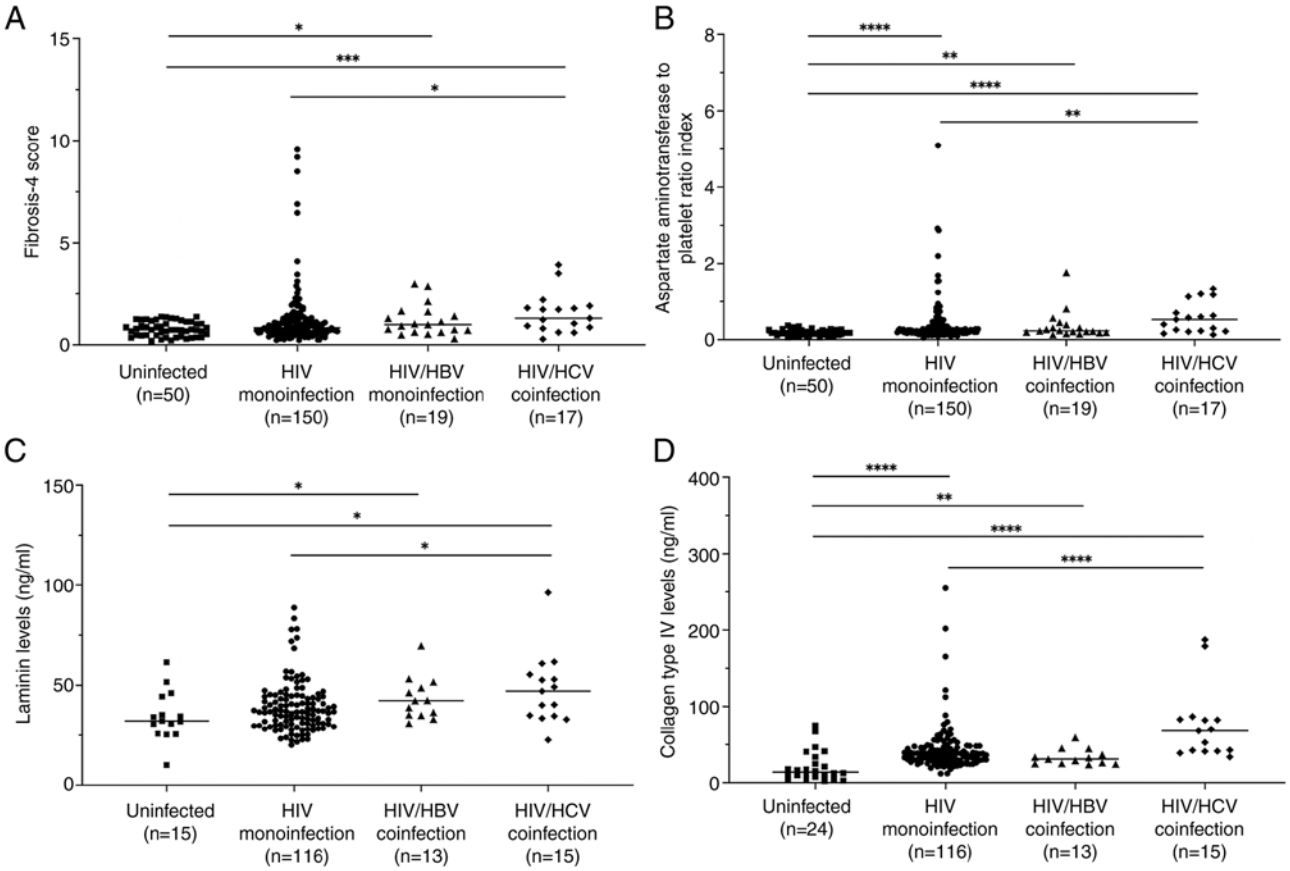


Figure 2. Non-invasive fibrosis marker measurement. (A) Fibrosis-4 score. (B) Aspartate aminotransferase to platelet ratio index. (C) Laminin and (D) type IV collagen levels. $^{*}$P<0.05, $^{**}$P<0.01, $^{***}$P<0.001 and $^{****}$P<0.0001. HIV, human immunodeficiency virus; HBV, hepatitis B virus; HCV, hepatitis C virus; NS, not significant.

RNA-binding protein 34, serine/threonine-protein kinase 31, E3 ubiquitin-protein ligase tripartite motif-containing 56, Mps one binder kinase activator 3C, E3 ubiquitin-protein ligase ring finger protein 220 and BRCA1-A complex subunit RAP80; six proteins were upregulated in the HIV/HBV group compared with the uninfected control group (116 kDa U5 small nuclear ribonucleoprotein component, nuclear cap-binding protein subunit 3, transmembrane channel-like protein 6, DNA replication ATP-dependent helicase/nuclease DNA 2, unconventional myosin-V and calpain-6). In addition, dual specificity calcium/calmodulin-dependent 3',5'-cyclic nucleotide phosphodiesterase was downregulated only in the HIV/HBV group and microtubule-associated protein 2 was upregulated only in the HIV-monoinfection group. The differential expression of these proteins suggests their potential roles in HIV monoinfection and coinfection with HBV and HCV.

*Association between 18 candidate proteins with profibrogenic, inflammatory and tumorigenic pathways*. To identify the molecular function of plasma protein profiles potentially associated with HIV infection and coinfection with HBV and HCV under long-term ART, the 18 selected proteins were analyzed for their interaction with proteins and chemicals in the STITCH 5.0 database (Fig. 4). Since accumulating evidence has indicated key roles of the profibrogenic TGF-β/SMAD and inflammatory TNF pathways in liver fibrogenesis and inflammation, especially in HIV and hepatotropic HBV and HCV (18,21,34,35), the proteins TGF-β, SMAD, TNF and ART drugs used in the patient groups (zidovudine, lamivudine, nevirapine and tenofovir) were included in the STITCH model. Input proteins serine/threonine kinase 31, chromosome 18 open reading frame 21, ring finger protein 220, myosin VA, tenascin XB, forkhead-associated, phosphopeptide binding domain 1, transmembrane channel-like 6, RNA binding motif protein 34, calpain 6, MOB kinase activator 3C, tripartite motif containing 56, microtubule-associated protein 2, nuclear cap binding protein subunit 1 and nuclear cap binding protein subunit 2 did not form any interaction with the protein networks. However, the model predicted close interactions between ubiquitin interaction motif containing 1 (UIMC1), also named BRCA1-A complex subunit RAP80, and BRCA1 and TGF-β/SMAD pathways. In addition, an interaction between haptoglobin (HP) and the TNF pathway was found. Notably, no protein exhibited interactions with ART drugs. Additionally, box plots indicated that the expression levels of UIMC1 and HP were 1.6-2.4 and 4.0-5.5 times lower in the three HIV-infected groups compared with those in the uninfected control group, who had no significant liver fibrosis, respectively. These results suggested the potential involvement of BRCA1-linked TGF-β/SMAD and TNF pathways during HIV-monoinfection and coinfection with HBV and HCV, in PLWH receiving suppressive ART.

Table II. Significantly differentially expressed proteins between HIV-monoinfected, HIV/hepatitis B/C virus-coinfected and uninfected controls.

| No. | Accession no. | Peptide sequence | Protein | False discovery rate | P-value |
|---|---|---|---|---|---|
| 1 | Q53F19 | AGSFITGIDVTSKEAIEK | Nuclear cap-binding protein subunit 3 | $1.06x10^{-14}$ | $9.89x10^{-18}$ |
| 2 | Q9Y6Q1 | DLRTYRR | Calpain-6 | $8.12x10^{-14}$ | $2.16x10^{-16}$ |
| 3 | P51530 | AVLSETFR | DNA replication ATP-dependent helicase/nuclease DNA 2 | $8.12x10^{-14}$ | $2.27x10^{-16}$ |
| 4 | Q5VTB9 | FEEYEWCGQKR | E3 ubiquitin-protein ligase RNF220 | $4.59x10^{-12}$ | $1.71x10^{-14}$ |
| 5 | Q32NC0 | GLHDSCPGQAR | UPF0711 protein C18orf21 (HBV X-transactivated gene 13 protein) | $5.01x10^{-12}$ | $2.33x10^{-14}$ |
| 6 | Q9Y4I1 | AACIRIQK | Unconventional myosin-Va | $1.35x10^{-11}$ | $7.56x10^{-14}$ |
| 7 | P22105 | DLRSGTLYSLTLYGLRGPHK | Tenascin-X | $4.23x10^{-11}$ | $2.75x10^{-13}$ |
| 8 | Q70IA8 | ALCLKQVFAKDK | MOB kinase activator 3C | $7.25x10^{-11}$ | $5.40x10^{-13}$ |
| 9 | P42696 | ESALASADLEEEIHQKQGQKR | RNA-binding protein 34 | $1.60x10^{-10}$ | $1.34x10^{-12}$ |
| 10 | Q9BXU1 | AATYHRAWR | Serine/threonine-protein kinase 31 | $3.09x10^{-10}$ | $2.87x10^{-12}$ |
| 11 | Q7Z403 | ELLAEWQLR | Transmembrane channel-like protein 6 | $3.39x10^{-10}$ | $3.46x10^{-12}$ |
| 12 | Q9BRZ2 | AAAAFAR | E3 ubiquitin-protein ligase TRIM56 | $6.87x10^{-10}$ | $7.67x10^{-12}$ |
| 13 | P11137 | AEKGLSSVPEIAEVEPSK | Microtubule-associated protein 2 | $5.70x10^{-8}$ | $6.90x10^{-10}$ |
| 14 | B1AJZ9 | AAGASGR | Forkhead-associated domain-containing protein 1 | $1.77x10^{-7}$ | $2.30x10^{-9}$ |
| 15 | Q15029 | AFIPAIDSFGFETDLR | 116 kDa U5 small nuclear ribonucleoprotein component | $1.81x10^{-7}$ | $2.53x10^{-9}$ |
| 16 | Q01064 | DWLASTFTQQARAKGR | Dual specificity calcium/calmodulin-dependent 3', 5'-cyclic nucleotide phosphodiesterase | $1.57x10^{-6}$ | $2.34x10^{-8}$ |
| 17 | Q96RL1 | ADQGDGPEGSGRACSTVEGK | BRCA1-A complex subunit RAP80 | $5.55x10^{-5}$ | $8.73x10^{-7}$ |
| 18 | P00738 | AVGDKLPECEADDGCPKPPEIAHGYVEHSVR | Haptoglobin (zonulin) | $3.62x10^{-3}$ | $6.07x10^{-4}$ |

HIV, human immunodeficiency virus.

## Discussion

Accumulating evidence suggests an increased burden of liver inflammation and fibrosis caused by HIV, HBV and HCV infection in PLWH (3,36,37). Previous cross-sectional studies in PLWH revealed a relatively high prevalence of liver fibrosis in patients with HBV or HCV coinfection (22,23). Due to accumulating evidence suggesting progression to more advanced CLD and HCC in PLWH with HBV/HCV (5,14-16), the present study aimed to examine the molecular changes in PLWH compared with virus-free uninfected controls. HIV-monoinfection, HIV/HBV and HIV/HCV groups had similar durations of ART, anti-retroviral drug regimens and immune status as assessed using the $CD4^+$ cell count. The uninfected control group had a similar median age to the HIV-infected groups and no significant liver fibrosis. The three HIV groups all showed significantly higher levels of liver fibrosis as evaluated using FIB-4 score and APRI, coupled with higher levels of extracellular matrix proteins LN and IVC, compared with the uninfected group; analysis also revealed higher levels of liver fibrosis in the HIV/HCV group compared with those in the HIV-monoinfection group. This was consistent with previous studies, indicating CLD in PLWH receiving ART and the influence of HCV infection in development of liver fibrosis in patients infected with HIV/HCV (5,11-16) The increased levels of liver fibrosis markers in HIV-infected

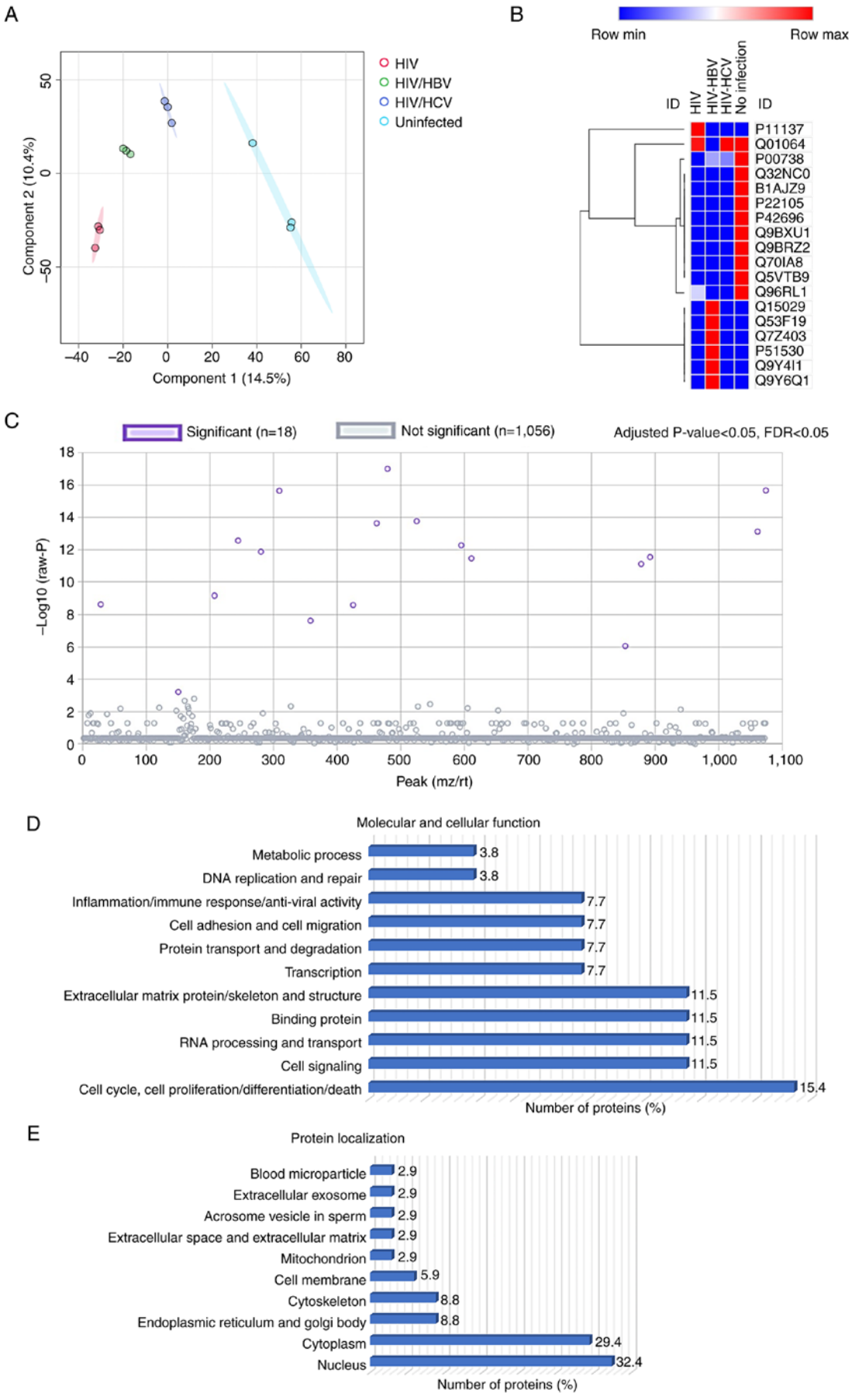


Figure 3. Bioinformatics analysis of 1,074 proteins identified by liquid chromatography-tandem mass spectrometry. (A) Partial least squares-discriminant analysis of protein abundance. (B) Heatmap analysis of 18 significantly differentially expressed proteins. Blue and red represent proteins with reduced and increased expression levels, respectively. (C) A total of 18 proteins had P-value and FDR<0.05. (D) Functional annotation and (E) subcellular distribution of the 18 selected proteins. HIV, human immunodeficiency virus; HBV, hepatitis B virus; HCV, hepatitis C virus; FDR, false discovery rate.

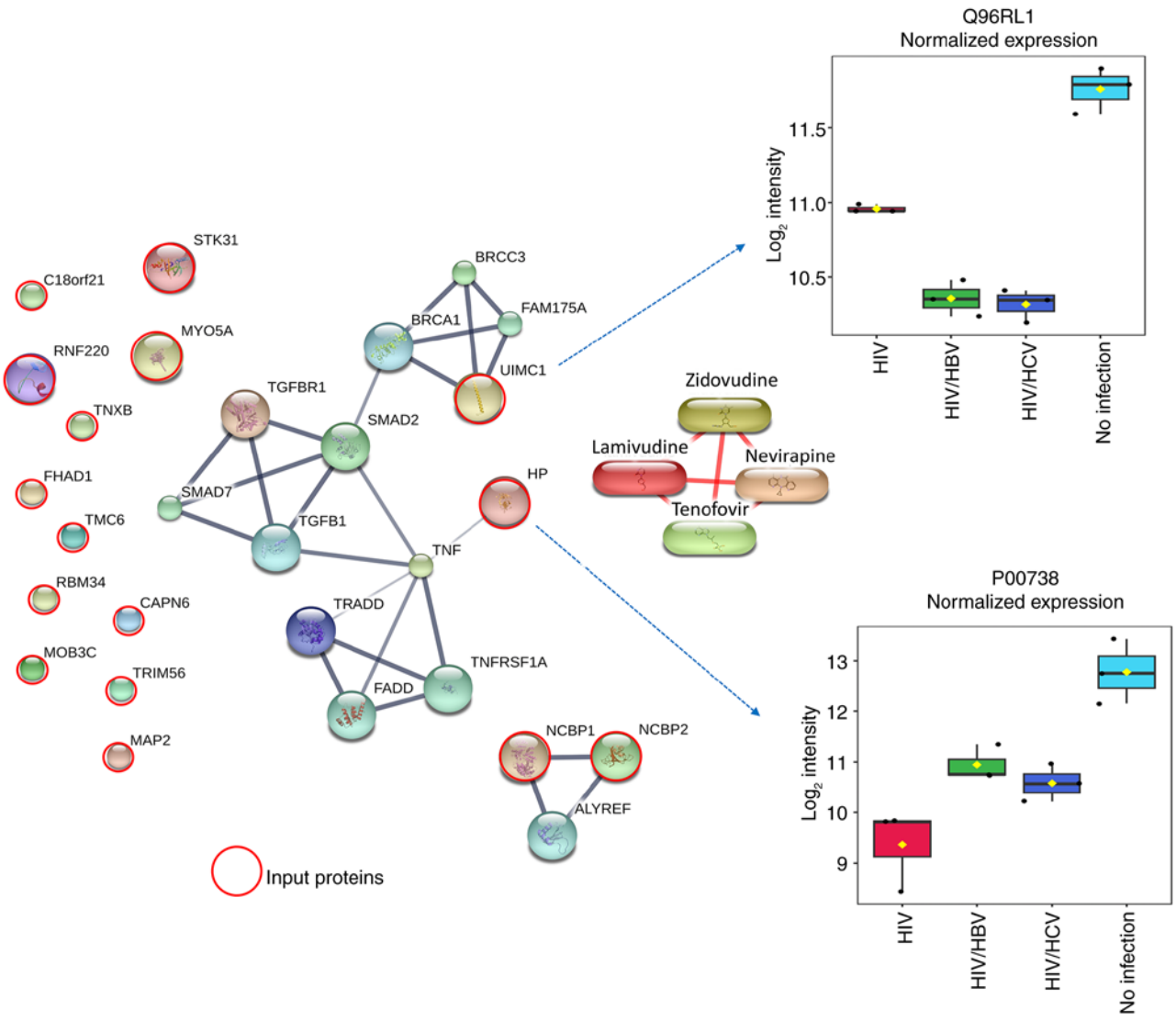


Figure 4. Protein-protein interaction network of TGF-1β/SMAD and TNF signaling pathways with HP and UIMC1. The model also predicted close interaction of UIMC1 with the BRCA1 pathway. Expression levels of proteins UIMC1) and P00738 (HP), are displayed beside the corresponding protein nodes in the model. Edges represent protein-protein interaction. A weaker association is represented by a thinner. HP, haptoglobin, UIMC1, ubiquitin interaction motif-containing 1, TRADD, TNFRSF1A-associated via death domain; HIV, human immunodeficiency virus; HBV, hepatitis B virus; HCV, hepatitis C virus.

groups may support potential progression to CLD in PLWH with HIV-monoinfection, HBV- and HCV-coinfection. Therefore, long-term monitoring of potential progression to advanced CLD is required in this study group.

The present study indicate differentially expression of the 18 candidate proteins suggesting their potential roles in the disease progression of HIV monoinfection and/or coinfection with HBV and HCV in PLWH and the functions of the candidate proteins were examined. Molecular functions of plasma proteins potentially associated with HIV monoinfection and coinfection with HBV and HCV in PLWH under long-term suppressive ART were predicted by STITCH 5.0 analysis. The STITCH model indicated no interaction between any candidate proteins with the four ARV drugs, suggesting no involvement of the proteins with mechanisms of the ARV drugs most commonly used in the HIV-moninfection group. However, the model revealed interactions between UIMC1 protein and BRCA1 and profibrogenic TGF-β/SMAD pathways, whereas an interaction was also found between HP and TNF pathways, which serve key roles in liver fibrogenesis and inflammation in HIV and hepatotropic HBV and HCV infection (18,21,34,35). Heatmap analysis and box plots demonstrated that these two proteins were downregulated in all HIV-infected groups compared with those in the uninfected control group. The analysis suggested potential involvement of BRCA1, TGF-β/SMAD and TNF pathways under of HIV-monoinfection and/or coinfection with HBV and HCV. In addition, novel protein targets UIMC1 and HP were identified to understand the molecular mechanisms of liver fibrosis in PLWH receiving suppressive ART.

UIMC1 or BRCA1-A complex subunit RAP80, a major contributor in the BRCA1 complex, functions in the DNA damage repair response (38,39). UIMC1 is a ubiquitin-binding protein targeting a complex containing BRCA1-BRCA1-associated ring domain protein 1 E3 ligase at double-strand breaks. This is required for DNA damage resistance, cell cycle checkpoint and DNA repair (40,41). *In vivo* study has indicated that loss of UIMC1 suppresses

recruitment of the BRCA1 complex to DNA damage sites and abolishes the repair process (42). BRCA1 is a tumor suppressor, the mutation or epigenetic inactivation of which increases the risk of various types of cancer, including HCC (43). To the best of our knowledge, there is a lack of direct evidence for an association between BRCA1 expression and liver disease caused by HIV and hepatotropic viruses. However, BRCA1/2 is one of the most commonly altered DNA damage repair genes associated with higher tumor mutation burden in patients diagnosed with primary liver cancer (44) and BRCA1 expression is associated with immune cell infiltration and proposed as a prognostic indicator of HCC (43). Here, the lower expression of UIMC1 in all three infected groups compared with that in uninfected groups may have impaired DNA repair response, potentially supporting tumourigenesis. HP is a secreted protein that has been reported to be an important regulator of intestinal barrier function (45,46). The HP pathway is involved in intestinal innate immunity and is dysregulated during chronic inflammatory diseases (45,46). HIV infection causes mucosal disruption in the gut, alteration of microbial composition and microbial translocation. These processes lead to chronic immune activation and inflammation, which are associated with non-AIDS comorbidities, including CLD (3). Consistent with the present study, previous studies have reported lower levels of serum HP in patients with chronic hepatitis B compared with controls (47) and an association between decreased HP levels with mortality in PLWH (48). However, increased serum levels of HP in more advanced liver disease are also reported (49,50). Accordingly, the lower expression of UIMC1 and HP proteins in all three infected groups compared with that in the uninfected control group, coupled with interactions with the profibrogenic TGF-β/SMAD, inflammatory TNF and tumor suppressor BRCA1 pathways, suggest potential roles of these proteins in liver inflammation and the progression to more advanced liver disease and HCC in PLWH.

The present study had limitations due to characteristics of the study groups and the cross-sectional design. The present study contained a relatively small number of subjects and information on their clinical symptoms was not obtained. In additon, there were significant differences in the sex distribution in the uninfected control and HIV-infected groups. However, in a previous study, multivariate analysis adjusted for different parameters suggested that sex was not a significant factor for liver fibrosis in PLWH (23). The influence of sex differences in the plasma protein profiles in the present study should be taken into account. There were also no specific treatments for HBV and HCV coinfection in any of the study groups, nor was the status of HBV and HCV infection, including HBV and HCV viral loads, available. Therefore, it remains unclear whether these parameters are associated with the protein profiles in the present study. To confirm the reliability of the protein profiles, the expression of candidate proteins, particularly UIMC1 and HP, should be validated and monitored in longitudinal studies. In addition, studies on the molecular and cellular functions of these proteins in the progression of HIV are warranted.

In conclusion, the present study was conducted on PLWH with HIV monoinfection or HBV and HCV coinfection receiving long-term ART. The comparative proteomics analysis revealed plasma protein profiles potentially associated with HIV infection, coinfection with HBV and HCV and liver fibrosis. STITCH model identified UIMC1 and HP proteins, which were associated with the profibrogenic TGF-β/SMAD, inflammatory TNF and tumor suppressor BRCA1 pathways, suggesting their potential role in inflammation, fibrosis and tumorigenesis in the liver. The proteomics data support the molecular basis of progressive liver disease in PLWH receiving long-term suppressive ART.

**Acknowledgements**

Not applicable.

**Funding**

The present study was supported by the Thailand Science Research and Innovation Fundamental Fund fiscal year 2022 (grant no. 2493097) and Thammasat University Research Unit in Diagnostic Molecular Biology of Chronic Diseases related to Cancer.

**Availability of data and materials**

The MS/MS raw data and analysis files have been deposited in the ProteomeXchange Consortium (proteomecentral.proteomexchange.org) via the jPOST partner repository (jpostdb.org) with the data set identifier JPST003189 and PXD PXD053504 (proteomecentral.proteomexchange.org/cgi/GetDataset?ID=PXD053504).

**Authors' contributions**

CA contributed to funding acquisition resources, supervision, study design, data analysis, manuscript preparation, review and editing. CT performed the experiments, data collection and analysis and manuscript preparation. JK conducted the detection of ECM fibrosis markers and tumor marker AFP and data analysis. TS and WS participated in blood samples and clinical data collection. NP and SR performed LC-MS/MS and data analysis. All authors read and approved the final version of the manuscript.

**Ethics approval and consent to participate**

The study protocol was approved by the Human Ethics Committees No. 3, Thammasat University (approval no. 116/2565) and Certificated Biological Safety Committee, Thammasat University, Pathumthani, Thailand. Written informed consent was obtained from the patients.

**Patient consent for publication**

Not applicable.

**Competing interests**

The authors declare that they have no competing interests.

## References


1. UNAIDS: Global HIV & AIDS statistics-Fact sheet. 2023.
2. Deeks SG, Lewin SR and Havlir DV: The end of AIDS: HIV infection as a chronic disease. Lancet 382: 1525-1533, 2013.
3. Zicari S, Sessa L, Cotugno N, Ruggiero A, Morrocchi E, Concato C, Rocca S, Zangari P, Manno EC and Palma P: Immune Activation, Inflammation, and Non-AIDS Co-Morbidities in HIV-Infected Patients under Long-Term ART. Viruses 11: 200, 2019.
4. Sherman KE and Thomas DL: HIV and liver disease: A comprehensive update. Top Antivir Med 30: 547-558, 2022.
5. Han WM, Ueaphongsukkit T, Chattranukulchai P, Siwamogsatham S, Chaiteerakij R, Sophonphan J, Gatechompol S, Ubolyam S, Phonphithak S, Ruxrungtham K, *et al*: Incident liver cirrhosis, associated factors, and cardiovascular disease risks among people living with HIV: A longitudinal study. J Acquir Immune Defic Syndr 86: 463-472, 2021.
6. Sun J, Althoff KN, Jing Y, Horberg MA, Buchacz K, Gill MJ, Justice AC, Rabkin CS, Goedert JJ, Sigel K, *et al*: Trends in Hepatocellular Carcinoma Incidence and Risk Among Persons With HIV in the US and Canada, 1996-2015. JAMA Netw Open 4: e2037512, 2021.
7. Torgersen J, Kallan MJ, Carbonari DM, Park LS, Mehta RL, D'Addeo K, Tate JP, Lim JK, Goetz MB, Rodriguez-Barradas MC, *et al*: HIV RNA, CD4+ Percentage, and Risk of Hepatocellular Carcinoma by Cirrhosis Status. J Natl Cancer Inst 112: 747-755, 2020.
8. Chamroonkul N and Bansal MB: HIV and the liver. Nat Rev Gastroenterol Hepatol 16: 1-2, 2019.
9. Ganesan M, Poluektova LY, Kharbanda KK and Osna NA: Human immunodeficiency virus and hepatotropic viruses co-morbidities as the inducers of liver injury progression. World J Gastroenterol 25: 398-410, 2019.
10. Sherman KE, Peters MG and Thomas D: Human immunodeficiency virus and liver disease: A comprehensive update. Hepatol Commun 1: 987-1001, 2017.
11. Mohr R, Schierwagen R, Schwarze-Zander C, Boesecke C, Wasmuth JC, Trebicka J and Rockstroh JK: Liver Fibrosis in HIV Patients Receiving a Modern cART: Which Factors Play a Role? Medicine (Baltimore) 94: e2127, 2015.
12. Rivero-Juarez A, Camacho A, Merchante N, Pérez-Camacho I, Macias J, Ortiz-Garcia C, Cifuentes C, Torre-Cisneros J, Peña J, Pineda JA, *et al*: Incidence of liver damage of uncertain origin in HIV patients not co-infected with HCV/HBV. PLoS One 8: e68953, 2013.
13. Sulyok M, Ferenci T, Makara M, Horváth G, Szlávik J, Rupnik Z, Kormos L, Gerlei Z, Sulyok Z and Vályi-Nagy I: Hepatic fibrosis and factors associated with liver stiffness in HIV mono-infected individuals. PeerJ 5: e2867, 2017.
14. Medrano LM, Garcia-Broncano P, Berenguer J, González-García J, Jiménez-Sousa MÁ, Guardiola JM, Crespo M, Quereda C, Sanz J, Canorea I, *et al*: Elevated liver stiffness is linked to increased biomarkers of inflammation and immune activation in HIV/hepatitis C virus-coinfected patients. AIDS 32: 1095-1105, 2018.
15. Portocarrero Nunez JA, Gonzalez-Garcia J, Berenguer J, Gallego MJV, Loyarte JAI, Metola L, Bernal E, Navarro G, Del Amo J and Jarrín I; and the Cohort of the Spanish HIV Research Network (CoRIS): Impact of co-infection by hepatitis C virus on immunological and virological response to antiretroviral therapy in HIV-positive patients. Medicine (Baltimore) 97: e12238, 2018.
16. Kim HN, Newcomb CW, Carbonari DM, Roy JA, Torgersen J, Althoff KN, Kitahata MM, Reddy KR, Lim JK, Silverberg MJ, *et al*: Risk of HCC With Hepatitis B Viremia Among HIV/HBV-Coinfected Persons in North America. Hepatology 74: 1190-1202, 2021.
17. Shmagel KV, Saidakova EV, Shmagel NG, Korolevskaya LB, Chereshnev VA, Robinson J, Grivel JC, Douek DC, Margolis L, Anthony DD and Lederman MM: Systemic inflammation and liver damage in HIV/hepatitis C virus coinfection. HIV Med 17: 581-589, 2016.
18. Shata MTM, Abdel-Hameed EA, Rouster SD, Yu L, Liang M, Song E, Esser MT, Shire N and Sherman KE: HBV and HIV/HBV infected patients have distinct immune exhaustion and apoptotic serum biomarker profiles. Pathog Immun 4: 39-65, 2019.
19. Lin W, Tsai WL, Shao RX, Wu G, Peng LF, Barlow LL, Chung WJ, Zhang L, Zhao H, Jang JY and Chung RT: Hepatitis C virus regulates transforming growth factor beta1 production through the generation of reactive oxygen species in a nuclear factor kappaB-dependent manner. Gastroenterology 138: 2509-2518, 2518 e1, 2010.
20. Salloum S, Holmes JA, Jindal R, Bale SS, Brisac C, Alatrakchi N, Lidofsky A, Kruger AJ, Fusco DN, Luther J, *et al*: Exposure to human immunodeficiency virus/hepatitis C virus in hepatic and stellate cell lines reveals cooperative profibrotic transcriptional activation between viruses and cell types. Hepatology 64: 1951-1968, 2016.
21. Ming D, Yu X, Guo R, Deng Y, Li J, Lin C, Su M, Lin Z and Su Z: Elevated TGF-β1/IL-31 pathway is associated with the disease severity of hepatitis B virus-related liver cirrhosis. Viral Immunol 28: 209-216, 2015.
22. Akekawatchai C, Sretapunya W, Pipatsatitpong D and Chuenchit T: Hepatitis B or C virus coinfection in and risks for transaminitis in human immunodeficiency virus-infected Thais on combined antiretroviral therapy. Asian Biomedicine 9: 353-361, 2015.
23. Chiraunyanann T, Changsri K, Sretapunya W, Yuenyongchaiwat K and Akekawatchai C: CXCL12 G801A polymorphism is associated with significant liver fibrosis in HIV-infected Thais: A cross-sectional study. Asian Pac J Allergy Immunol 37: 162-170, 2019.
24. Foca E, Fabbiani M, Prosperi M, Quiros Roldan E, Castelli F, Maggiolo F, Di Filippo E, Di Giambenedetto S, Gagliardini R, Saracino A, *et al*: Liver fibrosis progression and clinical outcomes are intertwined: Role of CD4+ T-cell count and NRTI exposure from a large cohort of HIV/HCV-coinfected patients with detectable HCV-RNA: A MASTER cohort study. Medicine (Baltimore) 95: e4091, 2016.
25. Sterling RK, Lissen E, Clumeck N, Sola R, Correa MC, Montaner J, S Sulkowski M, Torriani FJ, Dieterich DT, Thomas DL, *et al*: Development of a simple noninvasive index to predict significant fibrosis in patients with HIV/HCV coinfection. Hepatology 43: 1317-1325, 2006.
26. Wai CT, Greenson JK, Fontana RJ, Kalbfleisch JD, Marrero JA, Conjeevaram HS and Lok AS: A simple noninvasive index can predict both significant fibrosis and cirrhosis in patients with chronic hepatitis C. Hepatology 38: 518-526, 2003.
27. World Health Organization: Guidelines for the Care and Treatment of Persons Diagnosed with Chronic Hepatitis C Virus Infection. 2018.
28. Lowry OH, Rosebrough NJ, Farr AL and Randall RJ: Protein measurement with the Folin phenol reagent. J Biol Chem 193: 265-275, 1951.
29. Tyanova S, Temu T and Cox J: The MaxQuant computational platform for mass spectrometry-based shotgun proteomics. Nat Protoc 11: 2301-2319, 2016.
30. Howe EA, Sinha R, Schlauch D and Quackenbush J: RNA-Seq analysis in MeV. Bioinformatics 27: 3209-3210, 2011.
31. Pang Z, Zhou G, Ewald J, Chang L, Hacariz O, Basu N and Xia J: Using MetaboAnalyst 5.0 for LC-HRMS spectra processing, multi-omics integration and covariate adjustment of global metabolomics data. Nat Protoc 17: 1735-1761, 2022.
32. Starruss J, de Back W, Brusch L and Deutsch A: Morpheus: A user-friendly modeling environment for multiscale and multicellular systems biology. Bioinformatics 30: 1331-1332, 2014.
33. Dong H, Xu C, Zhou W, Liao Y, Cao J, Li Z and Hu B: The combination of 5 serum markers compared to FibroScan to predict significant liver fibrosis in patients with chronic hepatitis B virus. Clin Chim Acta 483: 145-150, 2018.
34. Dewidar B, Meyer C, Dooley S and Meindl-Beinker AN: TGF-β in hepatic stellate cell activation and liver fibrogenesis-updated 2019. Cells 8: 1419, 2019.
35. Steele H, Cheng J, Willicut A, Dell G, Breckenridge J, Culberson E, Ghastine A, Tardif V and Herro R: TNF superfamily control of tissue remodeling and fibrosis. Front Immunol 14: 1219907, 2023.
36. Demirkol ME, Aktas G, Bilgin S, Kahveci G, Kurtkulagi O, Atak BM and Duman TT: C-reactive protein to lymphocyte count ratio is a promising novel marker in hepatitis C infection: The clear hep-c study. Rev Assoc Med Bras (1992) 68: 838-841, 2022.
37. Kosekli MA: Mean platelet volume and platelet to lymphocyte count ratio are associated with hepatitis B-related liver fibrosis. Eur J Gastroenterol Hepatol 34: 324-327, 2022.

38. Anamika, Markin CJ, Rout MK and Spyracopoulos L: Molecular basis for impaired DNA damage response function associated with the RAP80 ΔE81 defect. J Biol Chem 289: 12852-12862, 2014.
39. Yan J, Kim YS, Yang XP, Li LP, Liao G, Xia F and Jetten AM: The ubiquitin-interacting motif containing protein RAP80 interacts with BRCA1 and functions in DNA damage repair response. Cancer Res 67: 6647-6656, 2007.
40. Sobhian B, Shao G, Lilli DR, Culhane AC, Moreau LA, Xia B, Livingston DM and Greenberg RA: RAP80 targets BRCA1 to specific ubiquitin structures at DNA damage sites. Science 316: 1198-1202, 2007.
41. Wang M, Gong Q, Zhang J, Chen L, Zhang Z, Lu L, Yu D, Han Y, Zhang D, Chen P, *et al*: Characterization of gene expression profiles in HBV-related liver fibrosis patients and identification of ITGBL1 as a key regulator of fibrogenesis. Sci Rep 7: 43446, 2017.
42. Wu J, Liu C, Chen J and Yu X: RAP80 protein is important for genomic stability and is required for stabilizing BRCA1-A complex at DNA damage sites in vivo. J Biol Chem 287: 22919-22926, 2012.
43. Mei J, Wang R, Xia D, Yang X, Zhou W, Wang H and Liu C: BRCA1 Is a novel prognostic indicator and associates with immune cell infiltration in hepatocellular carcinoma. DNA Cell Biol 39: 1838-1849, 2020.
44. Lin J, Shi J, Guo H, Yang X, Jiang Y, Long J, Bai Y, Wang D, Yang X, Wan X, *et al*: Alterations in DNA damage repair genes in primary liver cancer. Clin Cancer Res 25: 4701-4711, 2019.
45. Sturgeon C and Fasano A: Zonulin, a regulator of epithelial and endothelial barrier functions, and its involvement in chronic inflammatory diseases. Tissue Barriers 4: e1251384, 2016.
46. Fasano A: Zonulin and its regulation of intestinal barrier function: The biological door to inflammation, autoimmunity, and cancer. Physiol Rev 91: 151-175, 2011.
47. Calgin MK and Cetinkol Y: Decreased levels of serum zonulin and copeptin in chronic Hepatitis-B patients. Pak J Med Sci 35: 847-851, 2019.
48. Hunt PW, Sinclair E, Rodriguez B, Shive C, Clagett B, Funderburg N, Robinson J, Huang Y, Epling L, Martin JN, *et al*: Gut epithelial barrier dysfunction and innate immune activation predict mortality in treated HIV infection. J Infect Dis 210: 1228-1238, 2014.
49. Voulgaris TA, Karagiannakis D, Hadziyannis E, Manolakopoulos S, Karamanolis GP, Papatheodoridis G and Vlachogiannakos J: Serum zonulin levels in patients with liver cirrhosis: Prognostic implications. World J Hepatol 13: 1394-1404, 2021.
50. Wang X, Li MM, Niu Y, Zhang X, Yin JB, Zhao CJ and Wang RT: Serum Zonulin in HBV-Associated chronic hepatitis, liver cirrhosis, and hepatocellular carcinoma. Dis Markers 2019: 5945721, 2019.